

## Rational Assembly of Soluble Copper(II) Phosphonates: Synthesis, Structure and Magnetism of Molecular Tetranuclear Copper(II) Phosphonates<sup>#</sup>

Vadapalli Chandrasekhar,<sup>\*†</sup> Tapas Senapati,<sup>†</sup> Atanu Dey,<sup>†</sup> and E. Carolina Sañudo<sup>\*\*‡</sup>

<sup>†</sup>Department of Chemistry, Indian Institute of Technology Kanpur, Kanpur-208016, India, and <sup>‡</sup>Departament de Química Inorgànica and Institute for Nanoscience and Nanotechnology, Universitat de Barcelona, Diagonal 647, 08028 Barcelona, Spain

Received September 28, 2010

The reactions of the dinuclear copper complexes [Cu<sub>2</sub>(L)(OAc)] [H<sub>3</sub>L = *N,N'*-(2-hydroxypropane-1,3-diyl)bis(salicylaldehyde)] or [Cu<sub>2</sub>(L')(OAc)] (H<sub>3</sub>L' = *N,N'*-(2-hydroxypropane-1,3-diyl)bis(4,5-dimethylsalicylaldehyde)) with various phosphonic acids, RPO<sub>3</sub>H<sub>2</sub> (R = *t*-Bu, Ph, *c*-C<sub>5</sub>H<sub>9</sub>, *c*-C<sub>6</sub>H<sub>11</sub> or 2,4,6-*i*-Pr<sub>3</sub>-C<sub>6</sub>H<sub>2</sub>), leads to the replacement of the acetate bridge affording tetranuclear copper(II) phosphonates, [Cu<sub>4</sub>(L)<sub>2</sub>(*t*-BuPO<sub>3</sub>)](CH<sub>3</sub>OH)<sub>2</sub>(C<sub>6</sub>H<sub>6</sub>) (**1**), [Cu<sub>4</sub>(L)<sub>2</sub>(PhPO<sub>3</sub>)(H<sub>2</sub>O)<sub>2</sub>(NMe<sub>2</sub>CHO)](H<sub>2</sub>O)<sub>2</sub> (**2**), [Cu<sub>4</sub>(L')<sub>2</sub>(C<sub>5</sub>H<sub>9</sub>PO<sub>3</sub>)](CH<sub>3</sub>OH)<sub>2</sub> (**3**), [Cu<sub>4</sub>(L')<sub>2</sub>(C<sub>6</sub>H<sub>11</sub>PO<sub>3</sub>)(MeOH)<sub>4</sub>(H<sub>2</sub>O)<sub>2</sub> (**4**) and [Cu<sub>4</sub>(L')<sub>2</sub>(C<sub>30</sub>H<sub>46</sub>P<sub>2</sub>O<sub>5</sub>)](PhCH<sub>3</sub>) (**5**). The molecular structures of **1–4** reveal that a [RPO<sub>3</sub>]<sup>2-</sup> ligand is involved in holding the four copper atoms together by a 4.211 coordination mode. In **5**, an in situ formed [(RPO<sub>2</sub>)<sub>2</sub>O]<sup>4-</sup> ligand bridges two pairs of the dinuclear subunits. Magnetic studies on these complexes reveal that the phosphonate ligand is an effective conduit for magnetic interaction among the four copper centers present; a predominantly antiferromagnetic interaction is observed at low temperatures.

### Introduction

Organophosphonates [RPO<sub>3</sub>]<sup>2-</sup> and the related family of ligands have been attracting attention in recent years.<sup>1</sup> Many research groups, notably those of Clearfield and Zubieta, have pioneered the use of phosphonate ligands to assemble a large number of metal phosphonates that possess mainly extended structures (1D-coordination polymers, 2D-layered structures and 3D-pillared structures).<sup>2</sup> These compounds are of interest not only because of their structural and

compositional diversity but also because of their potential applications in various fields such as cation exchange,<sup>3</sup> sorption,<sup>4</sup> catalysis,<sup>5</sup> catalyst supports,<sup>5</sup> and sensors<sup>6</sup> as well as nonlinear optics.<sup>7</sup>

In contrast to metal phosphonates that possess extended structures, molecular metal phosphonates (zero-dimensional) are of recent origin and studies on these compounds

<sup>#</sup> Dedicated to Prof. Y. D. Vankar on his 60th birthday.

<sup>\*</sup>To whom correspondence should be addressed. E-mail: vc@iitk.ac.in (V.C.).

(1) (a) Cao, G.; Hong, G. H.; Mallouk, T. E. *Acc. Chem. Res.* **1992**, 25, 420. (b) Natarajan, S. S.; Mandal, S. *Angew. Chem. Int. Ed.* **2008**, 47, 4798. (c) Kong, D.; McBee, J. L.; Clearfield, A. *Cryst. Growth Des.* **2005**, 5, 643. (d) Kong, D.; Clearfield, A.; Zoiñ, J. *Cryst. Growth Des.* **2005**, 5, 1767. (e) Ouellette, W.; Wang, G.; Liu, H.; Yee, G. T.; O'Connor, C. J.; Zubieta, J. *Inorg. Chem.* **2009**, 48, 953.

(2) (a) Clearfield, A. *Curr. Opin. Solid State Mater. Sci.* **2002**, 6, 495. (b) Clearfield, A. *Curr. Opin. Solid State Mater. Sci.* **1996**, 1, 268. (c) Thompson, M. E. *Chem. Mater.* **1994**, 6, 1168. (d) Subbiah, A.; Pyle, D.; Rowland, A.; Huang, J.; Narayanan, R. A.; Thiyagarajan, P.; Zoiñ, J.; Clearfield, A. *J. Am. Chem. Soc.* **2005**, 127, 10826. (e) Song, S.-Y.; Ma, J.-F.; Yang, J.; Cao, M.-H.; Li, K.-C. *Inorg. Chem.* **2005**, 44, 2140. (f) Ouellette, W.; Yu, M. H.; O'Connor, C. J.; Zubieta, J. *Inorg. Chem.* **2006**, 45, 7628. (g) Ouellette, W.; Yu, M. H.; O'Connor, C. J.; Zubieta, J. *Inorg. Chem.* **2006**, 45, 3224. (h) Burkholder, E.; Golub, V.; O'Connor, C. J.; Zubieta, J. *Inorg. Chem.* **2004**, 43, 7014. (i) Yang, B.-P.; Mao, J.-G. *Inorg. Chem.* **2005**, 44, 566. (j) Clearfield, A. *Prog. Inorg. Chem.* **1998**, 47, 371. (k) Burkholder, E.; Golub, V.; O'Connor, C. J.; Zubieta, J. *Inorg. Chem.* **2003**, 42, 6729. (l) Yucesan, G.; Golub, V.; O'Connor, C. J.; Zubieta, J. *Dalton Trans.* **2005**, 2241. (m) Yucesan, G.; Golub, V.; O'Connor, C. J.; Zubieta, J. *CrystEngComm* **2004**, 6, 323. (n) Yucesan, G.; Yu, M. H.; Ouellette, W.; O'Connor, C. J.; Zubieta, J. *CrystEngComm* **2005**, 7, 480.

(3) (a) Clearfield, A. *Inorganic Ion Exchange Materials*, CRC Press, Boca Raton, FL, 1982. (b) Wang, J. D.; Clearfield, A.; Peng, G.-Z. *Mater. Chem. Phys.* **1993**, 35, 208. (c) Zangand, B.; Clearfield, A. *J. Am. Chem. Soc.* **1997**, 119, 2751.

(4) (a) Fredoueil, F.; Massiot, D.; Janvier, P.; Gingl, F.; Bujoli-Doeuff, M.; Evian, M.; Clearfield, A.; Bujoli, B. *Inorg. Chem.* **1999**, 38, 1831. (b) Maeda, K.; Kiyozumi, Y.; Mizukami, F. *J. Phys. Chem. B.* **1997**, 101, 4402. (c) Yue, Q.; Yang, J.; Li, G.-H.; Li, G.-D.; Chen, J.-S. *Inorg. Chem.* **2006**, 45, 4431. (d) Gallagher, L. A.; Serron, S. A.; Wen, X.; Hornstein, B. J.; Dattelbaum, D. M.; Schoonover, J. R.; Meyer, T. J. *Inorg. Chem.* **2005**, 44, 2089.

(5) (a) Wan, B.-Z.; Anthony, R. G.; Peng, G.-Z.; Clearfield, A. *J. Catal.* **1994**, 19, 101. (b) Deniaud, D.; Schollorn, B.; Mansury, J.; Rouxel, J.; Battion, P.; Bujoli, B. *Chem. Mater.* **1995**, 7, 995. (c) Hu, A.; Ngo, H.; Lin, W. *J. Am. Chem. Soc.* **2003**, 125, 11490. (d) Hu, A.; Yee, G. T.; Lin, W. *J. Am. Chem. Soc.* **2005**, 127, 12486. (e) Nonglaton, G.; Benitez, I. O.; Guisile, I.; Pipeler, M.; Leger, J.; Dubreuil, D.; Tellier, C.; Talham, D. R.; Bujoli, B. *J. Am. Chem. Soc.* **2004**, 126, 1497.

(6) (a) Ungashe, S. B.; Wilson, W. L.; Katz, H. E.; Scheller, G. R.; Putvinski, T. M. *J. Am. Chem. Soc.* **1992**, 114, 8717. (b) Sanchez-Moreno, M. J.; Fernandez-Botello, A.; Gomez-Coca, R. B.; Griesser, R.; Ochocki, J.; Kotynski, A.; Niclos-Gutierrez, J.; Moreno, V.; Sigel, H. *Inorg. Chem.* **2004**, 43, 1311. (c) Du, Z.-Y.; Xu, H.-B.; Mao, J.-G. *Inorg. Chem.* **2006**, 45, 6424.

(7) (a) Cabeza, A.; Aranda, M. A. G.; Bruque, S.; Poojary, D. M.; Clearfield, A.; Sanz, J. *Inorg. Chem.* **1998**, 37, 4168. (b) Zhang, B.; Poojary, D. M.; Clearfield, A. *Inorg. Chem.* **1998**, 37, 249. (c) Ayyappan, P.; Evans, O. R.; Cui, Y.; Wheeler, K. A.; Lin, W. *Inorg. Chem.* **2002**, 41, 4978.

have been limited.<sup>8</sup> One of the main reasons for this is that the multisite coordination capability of the phosphonate ligands generally leads to the formation of insoluble compounds.<sup>2</sup> Synthetically, this difficulty has been addressed by different strategies. We and others have used appropriate ancillary ligands which occupy and block a certain number of coordination sites on the transition metal ion.<sup>8</sup> As a result, the number of coordination sites that are accessible for the phosphonate ligand are limited and soluble products can be isolated. By using this methodology we had initially prepared a lipophilic dodecanuclear Cu(II) phosphonate cage,<sup>8a</sup> subsequently different types of molecular metal phosphonates with varying nuclearity have been assembled.<sup>8</sup> A second strategy is to use a sterically hindered lipophilic phosphonic acid with or without the use of an ancillary ligand.<sup>9</sup> Many main-group element phosphonates and transition metal phosphonates have been prepared by this method.<sup>9,10</sup> The combination of a sterically hindered phosphonic acid with an appropriate ancillary ligand is also an excellent method to limit the size of the metal phosphonate aggregate.<sup>11</sup> Most of these synthetic strategies, however, do not lead to predictable

assemblies. While the above synthetic methodology, also known as the serendipity approach<sup>12</sup> (because the final outcome of the product cannot be predicted), has a demonstrated utility, it is also important to come up with rational strategies that can lead to a predictable outcome. One promising approach that can lead to a rational outcome is the use of preformed metal aggregates as precursors. Reactions of trinuclear metal carboxylates  $[M_3O(O_2CR)_6(H_2O)_3] \cdot X$  ( $M = Mn, Fe, V, Cr$ ;  $R = H, CH_3, Ph, t-Bu$ ;  $X = NO_3^-, Cl^-$ ) with phosphonate ligands have been shown to generate larger metal aggregates although the size and structure of the latter still could not be predicted with certainty.<sup>13</sup> In view of our interest in molecular copper(II) phosphonates<sup>8a-g,j,k</sup> we were interested in exploring the use of precursors that would lead to a single predictable product. We reasoned that if the starting precursor had only one labile ligand, such as a carboxylate  $(RCO_2)^-$ , replacement of this with a phosphonate  $(RPO_3)^{2-}$  can lead to a controlled expansion of the size of the aggregate since the phosphonate ligand contains an additional donor oxygen to bind. We tested our hypothesis by the reaction of various phosphonic acids with two dinuclear copper(II) complexes  $\{[Cu_2(L)(OAc)](H_3L) (H_3L = 1,3-bis(salicylideneamino)propan-2-ol) \text{ and } [Cu_2(L')(OAc)](H_3L' = 1,3-bis(4,5-dimethylsalicylideneamino)propan-2-ol)\}$ ; the lability of the acetate ligand in these complexes has been demonstrated before.<sup>14</sup> Accordingly, in this manuscript we describe the synthesis, structural characterization and magnetic studies of the tetranuclear copper(II) phosphonates  $[Cu_4(L)_2(t-BuPO_3)](CH_3OH)_2(C_6H_6)$  (**1**),  $[Cu_4(L)_2(PhPO_3)(H_2O)_2(NMe_2CHO)](H_2O)_2$  (**2**),  $[Cu_4(L')_2(C_5H_9PO_3)](CH_3OH)_2$  (**3**),  $[Cu_4(L')_2(C_6H_{11}PO_3)](MeOH)_4(H_2O)_2$  (**4**) and  $[Cu_4(L')_2(C_{30}H_{46}P_2O_5)](PhCH_3)$  (**5**).

## Experimental Section

**Reagents and General Procedures.** All the reagents and the chemicals were purchased from commercial sources and were used without further purification. The compounds 1,3-bis(salicylideneamino)propan-2-ol ( $H_3L$ ),<sup>15</sup> 1,3-bis(4,5-dimethylsalicylideneamino)propan-2-ol ( $H_3L'$ )<sup>15</sup> (Scheme 1),  $t-BuPO_3 \cdot H_2O$ ,<sup>16</sup> cyclopentylphosphonic acid,<sup>16</sup> cyclohexylphosphonic

(8) (a) Chandrasekhar, V.; Kingsley, S. *Angew. Chem., Int. Ed.* **2000**, *39*, 2320. (b) Chandrasekhar, V.; Kingsley, S.; Vij, A.; Lam, K. C.; Rheingold, A. L. *Inorg. Chem.* **2000**, *39*, 3238. (c) Chandrasekhar, V.; Kingsley, S.; Rhatigan, B.; Lam, M. K.; Rheingold, A. L. *Inorg. Chem.* **2002**, *41*, 1030. (d) Chandrasekhar, V.; Nagarajan, L.; Clérac, R.; Ghosh, S.; Verma, S. *Inorg. Chem.* **2008**, *47*, 1067. (e) Chandrasekhar, V.; Azhakar, R.; Senapati, T.; Thilagar, P.; Ghosh, S.; Verma, S.; Boomishankar, R.; Steiner, A.; Kögerler, P. *Dalton Trans.* **2008**, 1150. (f) Chandrasekhar, V.; Nagarajan, L.; Clérac, R.; Ghosh, S.; Senapati, T.; Verma, S. *Inorg. Chem.* **2008**, *47*, 5347. (g) Chandrasekhar, V.; Senapati, T.; Sañudo, E. C. *Inorg. Chem.* **2008**, *47*, 9553. (h) Langley, S. J.; Helliwell, M.; Sessoli, R.; Rosa, P.; Wernsdorfer, W.; Wimpenny, R. E. P. *Chem. Commun.* **2005**, 5029. (i) Du, Z.-Y.; Li, X.-L.; Liu, Q.-Y.; Mao, J.-G. *Cryst. Growth Des.* **2007**, *7*, 1501. (j) Chandrasekhar, V.; Senapati, T.; Sañudo, E. C.; Clérac, R. *Inorg. Chem.* **2009**, *48*, 6192. (k) Chandrasekhar, V.; Senapati, T.; Clérac, R. *Eur. J. Inorg. Chem.* **2009**, 1640.

(9) (a) Baskar, V.; Shanmugam, M.; Sañudo, E. C.; Collison, D.; McInnes, E. J. L.; Wei, Q.; Wimpenny, R. E. P. *Chem. Commun.* **2007**, 37. (b) Khanra, S.; Klothe, M.; Mansaray, H.; Muryn, C. A.; Tuna, F.; Sañudo, E. C.; Helliwell, M.; McInnes, E. J. L.; Wimpenny, R. E. P. *Angew. Chem., Int. Ed.* **2007**, *46*, 5568. (c) Chandrasekhar, V.; Sasikumar, P.; Boomishankar, R.; Anantharaman, G. *Inorg. Chem.* **2006**, *45*, 3344.

(10) (a) Walawalkar, M. G.; Roesky, H. W.; Murugavel, R. *Acc. Chem. Res.* **1999**, *32*, 117. (b) Chakraborty, D.; Horchler, S.; Kraetzner, R.; Varkey, S. P.; Pinkas, J.; Roesky, H. W.; Uson, I.; Noltemeyer, M.; Schmidt, H.-G. *Inorg. Chem.* **2001**, *40*, 2620. (c) Walawalkar, M. G.; Murugavel, R.; Roesky, H. W.; Uson, I.; Kraetzner, R. *Inorg. Chem.* **1998**, *37*, 473. (d) Breeze, B. A.; Shanmugam, M.; Tuna, F.; Wimpenny, R. E. P. *Chem. Commun.* **2007**, 5185. (e) Walawalkar, M. G.; Murugavel, R.; Voigt, A.; Roesky, H. W.; Schmidt, H.-G. *J. Am. Chem. Soc.* **1997**, *119*, 4656. (f) Anantharaman, G.; Walawalkar, M. G.; Murugavel, R.; Gabor, B.; Herbst-Irmer, R.; Baldus, M.; Angerstein, B.; Roesky, H. W. *Angew. Chem., Int. Ed.* **2003**, *42*, 4482. (g) Yang, Y.; Pinkas, J.; Noltemeyer, M.; Schmidt, H.-G.; Roesky, H. W. *Angew. Chem., Int. Ed.* **1999**, *38*, 664. (h) Walawalkar, M. G.; Horchler, S.; Dietrich, S.; Chakraborty, D.; Roesky, H. W.; Schäfer, M.; Schmidt, H.-G.; Sheldrick, G. M.; Murugavel, R. *Organometallics* **1998**, *17*, 2865.

(11) (a) Chandrasekhar, V.; Sasikumar, P. *Dalton Trans.* **2008**, 6475. (b) Chandrasekhar, V.; Sasikumar, P.; Boomishankar, R. *Dalton Trans.* **2008**, 5189.

(12) (a) Wimpenny, R. E. P. *J. Chem. Soc., Dalton Trans.* **2002**, 1. (b) Parsons, S.; Wimpenny, R. E. P. *Acc. Chem. Res.* **1997**, *30*, 89. (c) Wimpenny, R. E. P. *Chem. Soc. Rev.* **1998**, *27*, 447. (d) Atkinson, I. M.; Benelli, C.; Murrie, M.; Parsons, S.; Wimpenny, R. E. P. *Chem. Commun.* **1999**, 285. (e) Mabbs, F. E.; McInnes, E. J. L.; Murrie, M.; Parsons, S.; Smith, G. M.; Wilson, C. C.; Wimpenny, R. E. P. *Chem. Commun.* **1999**, 643. (f) Parsons, S.; Smith, A. A.; Wimpenny, R. E. P. *Chem. Commun.* **1999**, 579. (g) Slagere, J. V.; Sessoli, R.; Gatteschi, D.; Smith, A. A.; Helliwell, M.; Wimpenny, R. E. P.; Cornia, A.; Barra, A.-L.; Jansen, A. G. M.; Rentschler, E.; Timco, G. A. *Chem.—Eur. J.* **2002**, *8*, 277. (h) Christian, P.; Rajaraman, G.; Harrison, A.; McDouall, J. J. W.; Raftery, J. T.; Wimpenny, R. E. P. *Dalton Trans.* **2004**, 1511. (i) Chandrasekhar, V.; Nagarajan, L.; Gopal, K.; Baskar, V.; Kögerler, P. *Dalton Trans.* **2005**, 3143. (j) Chandrasekhar, V.; Nagarajan, L. *Dalton Trans.* **2009**, 6712.

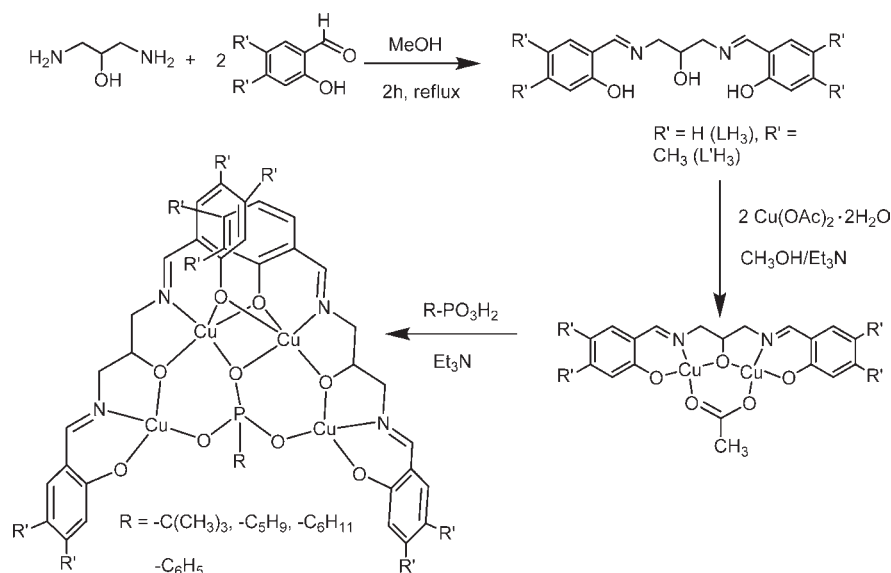
(13) (a) Figgis, B. N.; Robertson, G. B. *Nature* **1965**, *205*, 649. (b) Anzenhofer, K.; De Boer, J. J. *Recl. Trav. Chim. Pays-Bas* **1969**, *88*, 286. (c) Hessel, L. W.; Romers, C. *Recl. Trav. Chim. Pays-Bas* **1969**, *88*, 545. (d) Blake, A. B.; Fraser, L. R. *Dalton Trans.* **1975**, 193. (e) Castro, S. L.; Streib, W. E.; Sun, J.-S.; Chritou, G. *Inorg. Chem.* **1996**, *35*, 4462. (f) Ribas, J.; Albela, B.; Stoeckli-Evans, H.; Chritou, G. *Inorg. Chem.* **1997**, *36*, 2352. (g) Wu, R.; Poyraz, M.; Sowrey, F. E.; Anson, C. E.; Wocadlo, S.; Powell, A. K.; Jayasooriya, U. A.; Cannon, R. D.; Nakamoto, T.; Katada, M.; Sano, H. *Inorg. Chem.* **1998**, *37*, 1913. (h) Brechin, E. K.; Coxall, R. A.; Parkin, A.; Parsons, S.; Taskar, P. A.; Wimpenny, R. E. P. *Angew. Chem., Int. Ed.* **2001**, *40*, 2700. (i) Shanmugam, M.; Shanmugam, M.; Chastanet, G.; Sessoli, R.; Mallah, T.; Wernsdorfer, W.; Wimpenny, R. E. P. *J. Mater. Chem.* **2006**, *16*, 2576. (j) Shanmugam, M.; Chastanet, G.; Mallah, T.; Sessoli, R.; Teat, S. J.; Timco, G. A.; Wimpenny, R. E. P. *Chem.—Eur. J.* **2006**, *12*, 8777. (k) Shanmugam, M.; Chastanet, G.; Teat, S. J.; Mallah, T.; Sessoli, R.; Wernsdorfer, W.; Wimpenny, R. E. P. *Angew. Chem., Int. Ed.* **2005**, *44*, 5044. (l) Tolis, E. I.; Helliwell, M.; Langley, S.; Raftery, J.; Wimpenny, R. E. P. *Angew. Chem., Int. Ed.* **2003**, *42*, 3804.

(14) (a) Mukherjee, A.; Saha, M. K.; Rudra, I.; Ramasesha, S.; Nethaji, M.; Chakravarty, A. R. *Inorg. Chim. Acta* **2004**, *357*, 1077. (b) Mukherjee, A.; Saha, M. K.; Nethaji, M.; Chakravarty, A. R. *Polyhedron* **2004**, *23*, 2177. (c) Geetha, K.; Tiwary, S. K.; Chakravarty, A. R.; Ananthakrishna, G. *J. Chem. Soc., Dalton Trans.* **1999**, 4463.

(15) Nishida, Y.; Kida, S. *J. Chem. Soc., Dalton Trans.* **1986**, 2633.

(16) (a) Crofts, P. C.; Kosolapoff, G. M. *J. Am. Chem. Soc.* **1953**, *75*, 3379. (b) Bengelsdorf, I. S.; Barron, L. B. *J. Am. Chem. Soc.* **1955**, *77*, 2869.

(17) Whitesides, G. M.; Eisenhut, M.; Bunting, W. M. *J. Am. Chem. Soc.* **1974**, *96*, 5399.

Scheme 1. Synthesis of 1–4<sup>a</sup>

<sup>a</sup> 1: R = *t*-Bu, 2: R = C<sub>6</sub>H<sub>5</sub>, 3: R = C<sub>5</sub>H<sub>9</sub>, 4: R = C<sub>6</sub>H<sub>11</sub>.

acid,<sup>16</sup> 2,4,6-tri-isopropylphenylphosphonic acid<sup>9c,17</sup> and the dinuclear copper(II) complexes [Cu<sub>2</sub>(L)(OAc)] and [Cu<sub>2</sub>(L')(OAc)]<sup>15</sup> were prepared by using procedures that were reported in the literature. Solvents were purified by conventional methods.<sup>18</sup> The following chemicals were used as received: *t*-BuOH (s. d. Fine Chemicals, India), Cu(OAc)<sub>2</sub> · 2H<sub>2</sub>O (Fluka, Switzerland), AlCl<sub>3</sub> (s. d. Fine Chemicals, India), PCl<sub>3</sub> (s. d. Fine Chemicals, India), 1,3-diaminopropan-2-ol (Fluka, Switzerland), salicylaldehyde (Fluka, Switzerland), 4,5-dimethylsalicylaldehyde (Fluka, Switzerland) and phenylphosphonic acid (Fluka, Switzerland).

**Instrumentation.** Melting points were measured using a JSGW melting point apparatus and are uncorrected. Electronic spectra were recorded on a Perkin-Elmer-Lambda 20 UV–vis spectrometer and on a Shimadzu UV-160 spectrometer using methanol as the solvent. IR spectra were recorded as KBr pellets on a Bruker Vector 22 FT IR spectrophotometer operating between 400 and 4000 cm<sup>-1</sup>. Elemental analyses of the compounds were obtained using a Thermoquest CE instrument CHNS-O, EA/110 model. ESI-MS analyses were performed on a Waters Micromass Quattro Micro triple quadrupole mass spectrometer. The ionization mechanism used was electrospray in positive ion full scan mode using methanol as the solvent; nitrogen gas was used for desolvation. Capillary voltage was maintained at 3 kV, and cone voltage was kept at 30 V. The temperature maintained for ion source was 100 °C and for desolvation 250 °C. <sup>1</sup>H and <sup>31</sup>P{<sup>1</sup>H} NMR spectra were recorded in CD<sub>3</sub>OD solutions on a JEOL JNM LAMBDA 400 model spectrometer operating at 400.0 and 161.7 MHz respectively. Chemical shifts are reported in ppm and are referenced with respect to internal tetramethylsilane (<sup>1</sup>H) and external 85% H<sub>3</sub>PO<sub>4</sub> (<sup>31</sup>P).

**Magnetic Measurements.** Magnetic data were collected at the Unitat de Mesures Magnètiques at the Universitat de Barcelona using crushed crystals of the sample on a Quantum Design MPMS-XL SQUID magnetometer equipped with a 5 T magnet. The data were corrected for TIP, and the diamagnetic corrections were calculated using Pascal's constants; an experimental correction for the sample holder was applied.

**Synthesis. General Synthetic Procedure Used for the Preparation of 1–5.** Dinuclear copper complexes [Cu<sub>2</sub>(L)(OAc)]

(H<sub>3</sub>L = *N,N'*-(2-hydroxypropane-1,3-diyl)bis(salicylaldehyde) or [Cu<sub>2</sub>(L')(OAc)] (H<sub>3</sub>L' = *N,N'*-(2-hydroxypropane-1,3-diyl)bis(4,5-dimethylsalicylaldehyde) were reacted with appropriate phosphonic acids, RPO<sub>3</sub>H<sub>2</sub> (R = *t*-Bu, Ph, *c*-C<sub>5</sub>H<sub>9</sub>, *c*-C<sub>6</sub>H<sub>11</sub> or 2,4,6-*i*-Pr<sub>3</sub>-C<sub>6</sub>H<sub>2</sub>) in the presence of triethylamine in methanol (30 mL) for a period of 12 h at room temperature. A clear deep green-colored solution was obtained. This was completely evaporated in vacuum. The resultant green solid was redissolved [dichloromethane/benzene (10:1) for **1**, methanol/dimethylformamide (15:1) for **2**, methanol/acetonitrile (10:1) for **3**, methanol/chloroform (5:1) for **4**, methanol/toluene (10:1) for **5**], filtered, and left undisturbed to allow crystallization. After 2–3 weeks block-shaped blue-colored crystals were obtained.

[Cu<sub>4</sub>(L)<sub>2</sub>(*t*-BuPO<sub>3</sub>)](CH<sub>3</sub>OH)<sub>2</sub>(C<sub>6</sub>H<sub>6</sub>) (**1**). Quantities: [Cu<sub>2</sub>(L)(OAc)] (0.200 g, 0.420 mmol), *t*-BuPO<sub>3</sub>H<sub>2</sub> (0.029 g, 0.210 mmol) and triethylamine (0.021 g, 0.420 mmol). Yield: 0.153 g, 67% (based on metal). Mp: 246 °C (dec). UV–vis (CH<sub>3</sub>OH) λ<sub>max</sub>/nm (ε/L mol<sup>-1</sup> cm<sup>-1</sup>): 648 (376). FT-IR ν/cm<sup>-1</sup>: 3396 (b), 2927 (b), 1637 (s), 1600 (m), 1537 (s), 1470 (m), 1450 (s), 1398 (m), 1312 (m), 1150 (s), 986 (s), 892 (s), 886 (m), 794 (s), 756 (s), 599 (m), 463 (m). ESI-MS *m/z*, ion: 980.96 [{Cu<sub>4</sub>(L)<sub>2</sub>(*t*-BuPO<sub>3</sub>)} + H]<sup>+</sup>. Anal. Calcd for C<sub>43</sub>H<sub>52</sub>Cu<sub>4</sub>N<sub>4</sub>O<sub>12</sub>P: C, 46.86; H, 4.76; N, 5.08. Found: C, 46.88; H, 4.87; N, 5.04.

[Cu<sub>4</sub>(L)<sub>2</sub>(PhPO<sub>3</sub>)](H<sub>2</sub>O)<sub>2</sub>(NMe<sub>2</sub>CHO)](H<sub>2</sub>O)<sub>2</sub> (**2**). Quantities: [Cu<sub>2</sub>(L)(OAc)] (0.200 g, 0.420 mmol), PhPO<sub>3</sub>H<sub>2</sub> (0.033 g, 0.210 mmol) and triethylamine (0.022 g, 0.42 mmol). Yield: 0.165 g, 70% (based on metal). Mp: 256 °C (dec). UV–vis (CH<sub>3</sub>OH) λ<sub>max</sub>/nm (ε/L mol<sup>-1</sup> cm<sup>-1</sup>): 652 (385). FT-IR ν/cm<sup>-1</sup>: 3466 (b), 3042 (m), 2918 (m), 1635 (s), 1599 (m), 1536 (m), 1450 (s), 1338 (m), 1253 (s), 1131 (s), 1061 (m), 996 (m), 890 (m), 791 (s), 717 (m), 684 (m), 576 (m). ESI-MS *m/z*, ion: 1000.94 [{Cu<sub>4</sub>(L)<sub>2</sub>(PhPO<sub>3</sub>)} + H]<sup>+</sup>. Anal. Calcd for C<sub>43</sub>H<sub>35</sub>Cu<sub>4</sub>N<sub>5</sub>O<sub>14</sub>P: C, 45.67; H, 3.12; N, 6.19. Found: C, 45.88; H, 3.16; N, 6.14.

[Cu<sub>4</sub>(L')<sub>2</sub>(*c*-C<sub>5</sub>H<sub>9</sub>PO<sub>3</sub>)](CH<sub>3</sub>OH)<sub>2</sub> (**3**). Quantities: [Cu<sub>2</sub>(L')(OAc)] (0.144 g, 0.268 mmol), *c*-C<sub>5</sub>H<sub>9</sub>PO<sub>3</sub>H<sub>2</sub> (0.020 g, 0.134 mmol) and triethylamine (0.027 g, 0.268 mmol). Yield: 0.098 g, 62% (based on metal). Mp: 260 °C (dec). UV–vis (CH<sub>3</sub>OH) λ<sub>max</sub>/nm (ε/L mol<sup>-1</sup> cm<sup>-1</sup>): 650 (703). FT-IR ν/cm<sup>-1</sup>: 3423 (b), 2917 (m), 2860 (m), 1630 (s), 1515 (s), 1475 (m), 1453 (s), 1392 (s), 1279 (s), 1226 (m), 1180 (m), 1147 (m), 1118 (m), 1062 (s), 964 (s), 881 (m), 861 (m), 779 (s), 678 (s), 589 (m), 518 (m), 468 (m). ESI-MS *m/z*, ion: 1105.098 [{Cu<sub>4</sub>(L')<sub>2</sub>(C<sub>5</sub>H<sub>9</sub>PO<sub>3</sub>)} + H]<sup>+</sup>. Anal.

(18) Vogel's Textbook of Practical Organic Chemistry, 5th ed.; Longman: London, 1989.

Table 1. Crystal Data and Structure Refinement Parameters of 1–5

parameters	1	2	3	4	5
empirical formula	C <sub>43</sub> H <sub>52</sub> Cu <sub>4</sub> N <sub>4</sub> O <sub>12</sub> P	C <sub>43</sub> H <sub>35</sub> Cu <sub>4</sub> N <sub>5</sub> O <sub>14</sub> P	C <sub>49</sub> H <sub>63</sub> Cu <sub>4</sub> N <sub>4</sub> O <sub>11</sub> P	C <sub>52</sub> H <sub>69</sub> Cu <sub>4</sub> N <sub>4</sub> O <sub>15</sub> P	C <sub>79</sub> H <sub>99</sub> Cu <sub>4</sub> N <sub>4</sub> O <sub>11</sub> P <sub>2</sub>
formula weight	1102.02	1130.89	1169.16	1275.29	1596.77
temp (K)	100(2)	173(2)	100(2)	100(2)	100(2)
wavelength (Å)	0.71073	0.71073	0.71069	0.71069	0.71069
cryst syst, space group	orthorhombic, <i>Pbca</i>	monoclinic, <i>P2<sub>1</sub>/c</i>	triclinic, <i>P1</i>	triclinic, <i>P1</i>	triclinic, <i>P1</i>
unit cell dimens					
<i>a</i> (Å)	20.533(10)	13.841(2)	11.927(5)	13.168(5)	15.806(5)
<i>b</i> (Å)	18.225(9)	33.287(5)	14.305(5)	14.028(5)	16.854(5)
<i>c</i> (Å)	24.150(12)	10.577(16)	16.632(5)	16.709(5)	17.237(5)
$\alpha$ (deg)	90	90	74.943(5)	75.594(5)	68.379(5)
$\beta$ (deg)	90	107.414(3)	75.092(5)	76.835(5)	86.815(5)
$\gamma$ (deg)	90	90	68.735(5)	67.154(5)	64.470(5)
vol (Å <sup>3</sup> )	9037.3(8)	4649.9(12)	2511.4(16)	2725.0(16)	3823(2)
Z, calcd density (mg/m <sup>3</sup> )	8, 1.620	4, 1.615	2, 1.546	2, 1.554	2, 1.387
abs coeff	1.959 mm <sup>-1</sup>	1.910 mm <sup>-1</sup>	1.765 mm <sup>-1</sup>	1.639 mm <sup>-1</sup>	1.201 mm <sup>-1</sup>
<i>F</i> (000)	4520	2284	1208	1320	1670
cryst size (mm <sup>3</sup> )	0.30 × 0.20 × 0.10	0.16 × 0.10 × 0.05	0.21 × 0.19 × 0.15	0.6 × 0.5 × 0.3	0.30 × 0.20 × 0.10
$\theta$ range for data collection	1.98 to 28.32°	1.97 to 28.32°	2.03 to 26.00°	2.22 to 25.50°	2.04 to 25.50°
limiting indices	-27 ≤ <i>h</i> ≤ 27, -24 ≤ <i>k</i> ≤ 24, -16 ≤ <i>l</i> ≤ 32	-15 ≤ <i>h</i> ≤ 18, -43 ≤ <i>k</i> ≤ 44, -13 ≤ <i>l</i> ≤ 13	-14 ≤ <i>h</i> ≤ 12, -15 ≤ <i>k</i> ≤ 17, -18 ≤ <i>l</i> ≤ 20	-15 ≤ <i>h</i> ≤ 14, -16 ≤ <i>k</i> ≤ 13, -20 ≤ <i>l</i> ≤ 20	-17 ≤ <i>h</i> ≤ 19, -16 ≤ <i>k</i> ≤ 20, -20 ≤ <i>l</i> ≤ 20
reflns collected/unique	57925/11242 [ <i>R</i> <sub>int</sub> = 0.0768]	30571/11428 [ <i>R</i> <sub>int</sub> = 0.0619]	14038/9639 [ <i>R</i> <sub>int</sub> = 0.0493]	14319/9886 [ <i>R</i> <sub>int</sub> = 0.0329]	20508/13909 [ <i>R</i> <sub>int</sub> = 0.0332]
completeness to $\theta$	99.8%	98.6%	97.5%	97.6%	97.7%
data/restraints/params	11242/1/571	11428/0/593	9639/0/637	9886/0/701	13909/0/921
goodness-of-fit on <i>F</i> <sup>2</sup>	1.035	1.038	1.025	1.041	1.026
final <i>R</i> indices [ <i>I</i> > 2 $\sigma$ ( <i>I</i> )]	<i>R</i> 1 = 0.0564, w <i>R</i> 2 = 0.1306	<i>R</i> 1 = 0.0630, w <i>R</i> 2 = 0.1523	<i>R</i> 1 = 0.0915, w <i>R</i> 2 = 0.2194	<i>R</i> 1 = 0.0839, w <i>R</i> 2 = 0.2275	<i>R</i> 1 = 0.0567, w <i>R</i> 2 = 0.1343
<i>R</i> indices (all data)	<i>R</i> 1 = 0.0819, w <i>R</i> 2 = 0.1432	<i>R</i> 1 = 0.1197, w <i>R</i> 2 = 0.1997	<i>R</i> 1 = 0.1562, w <i>R</i> 2 = 0.2674	<i>R</i> 1 = 0.1228, w <i>R</i> 2 = 0.2660	<i>R</i> 1 = 0.0807, w <i>R</i> 2 = 0.1532
largest diff. peak and hole (e <sup>-</sup> Å <sup>-3</sup> )	1.693 and -0.707	1.138 and -0.694	1.177 and -0.726	1.711 and -1.139	0.969 and -0.621

Calcd for C<sub>49</sub>H<sub>63</sub>Cu<sub>4</sub>N<sub>4</sub>O<sub>11</sub>P: C, 50.34; H, 5.43; N, 4.79. Found: C, 50.21; H, 5.12; N, 4.20.

[Cu<sub>2</sub>(L')<sub>2</sub>(c-C<sub>6</sub>H<sub>11</sub>PO<sub>3</sub>)(MeOH)<sub>4</sub>(H<sub>2</sub>O)<sub>2</sub>] (4). Quantities: [Cu<sub>2</sub>(L')(OAc)] (0.120 g, 0.22 mmol), c-C<sub>6</sub>H<sub>11</sub>PO<sub>3</sub>H<sub>2</sub> (0.019 g, 0.115 mmol) and triethylamine (0.022 g, 0.22 mmol). Yield: 0.078 g, 55% (based on metal). Mp: 264 °C (dec). UV-vis (CH<sub>3</sub>-OH)  $\lambda_{\max}$ /nm ( $\epsilon$ /L mol<sup>-1</sup> cm<sup>-1</sup>): 650 (816). FT-IR  $\nu$ /cm<sup>-1</sup>: 3416 (b), 2917 (m), 2852 (m), 1629 (s), 1516 (s), 1475 (m), 1453 (s), 1392 (s), 1343 (m), 1278 (s), 1227 (m), 1181 (m), 1138 (s), 1118 (s), 1061 (s), 960 (s), 858 (m), 779 (s), 682 (s), 589 (m), 519 (m). ESI-MS *m/z*, ion: 1119.11 [(Cu<sub>4</sub>(L')<sub>2</sub>(C<sub>6</sub>H<sub>11</sub>PO<sub>3</sub>)<sub>2</sub> + H)<sup>+</sup>]. Anal. Calcd for C<sub>52</sub>H<sub>77</sub>Cu<sub>4</sub>N<sub>4</sub>O<sub>15</sub>P: C, 48.67; H, 6.05; N, 4.37. Found: C, 48.28; H, 6.06; N, 4.14.

[Cu<sub>4</sub>(L')<sub>2</sub>(2,4,6-*i*-Pr<sub>3</sub>-C<sub>6</sub>H<sub>2</sub>PO<sub>2</sub>)<sub>2</sub>O](PhCH<sub>3</sub>) (5). Quantities: [Cu<sub>2</sub>(L')(OAc)] (0.142 g, 0.264 mmol), 2,4,6-*i*-Pr<sub>3</sub>-C<sub>6</sub>H<sub>2</sub>PO<sub>3</sub>H<sub>2</sub> (0.038 g, 0.132 mmol) and triethylamine (0.027 g, 0.264 mmol). Yield: 0.123 g, 58% (based on metal). Mp: 274 °C (dec). UV-vis (CH<sub>3</sub>OH)  $\lambda_{\max}$ /nm ( $\epsilon$ /L mol<sup>-1</sup> cm<sup>-1</sup>): 635 (642). FT-IR  $\nu$ /cm<sup>-1</sup>: 3430 (b), 2957 (m), 2919 (m), 2862 (m), 1630 (s), 1569 (m), 1512 (s), 1456 (m), 1394 (m), 1275 (m), 1250 (m), 1181 (s), 1062 (m), 999 (m), 867 (s), 778 (s), 732 (m), 666 (m), 583 (m), 517 (s), 469 (m), 431 (m). ESI-MS *m/z*, ion: 1505.35 [(Cu<sub>4</sub>(L')<sub>2</sub>(2,4,6-*i*-Pr<sub>3</sub>-C<sub>6</sub>H<sub>2</sub>PO<sub>2</sub>)<sub>2</sub>O) + H)<sup>+</sup>]. Anal. Calcd for C<sub>79</sub>H<sub>100</sub>Cu<sub>4</sub>N<sub>4</sub>O<sub>11</sub>P<sub>2</sub>: C, 59.38; H, 6.31; N, 3.51. Found: C, 59.18; H, 6.16; N, 3.34.

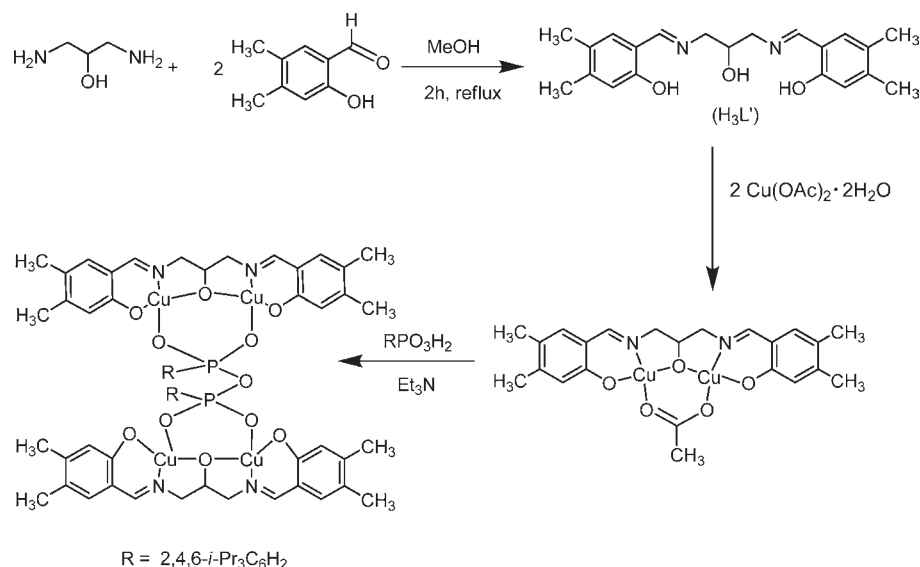
**X-ray Crystallography.** The crystal data and the cell parameters for compounds 1–5 are given in Table 1. Single crystals suitable for X-ray crystallographic analyses were obtained by

slow evaporation of dichloromethane/benzene (1), methanol/DMF (2) methanol/acetonitrile (10:1) (3), methanol/chloroform (5:1) (4) or methanol/toluene (10:1) (5) solutions. The crystal data for compounds 1–5 have been collected on a Bruker SMART CCD diffractometer using a Mo K $\alpha$  sealed tube. The program SMART<sup>19a</sup> was used for collecting frames of data, indexing reflections, and determining lattice parameters, SAINT<sup>19a</sup> for integration of the intensity of reflections and scaling, SADABS<sup>19b</sup> for absorption correction, and SHELXTL<sup>19c,d</sup> for space group and structure determination and least-squares refinements on *F*<sup>2</sup>. All the structures were solved by direct methods using the program SHELXS-97<sup>13e</sup> and refined by full-matrix least-squares methods against *F*<sup>2</sup> with SHELXL-97.<sup>19e</sup> Hydrogen atoms were fixed at calculated positions, and their positions were refined by a riding model. All non-hydrogen atoms were refined with anisotropic displacement parameters. The disordered water molecules were refined isotropically. The crystallographic figures have been generated using Diamond 3.1e software.<sup>19f</sup>

## Results and Discussion

**Synthetic Aspects.** Two dinuclear copper complexes [Cu<sub>2</sub>(L)(OAc)] and [Cu<sub>2</sub>(L')(OAc)] were prepared by the reaction of H<sub>3</sub>L and H<sub>3</sub>L' with Cu(OAc)<sub>2</sub>·2H<sub>2</sub>O respectively (Schemes 1 and 2). The unique structural feature of the deprotonated trianionic ligand platform (L<sup>3-</sup> or L'<sup>3-</sup>) allows the encapsulation of two copper centers. The two copper atoms are bridged by a  $\mu$ -O as well as a  $\mu$ -acetate. An examination of these complexes reveals that the dinuclear copper framework is quite robust; on the other hand the acetate bridge is the weak link and can be replaced by other ligands.<sup>14</sup> We reasoned that replacing the bidentate acetate ligand in these dinuclear complexes with the potentially multidentate phosphonate ligand, [RPO<sub>3</sub>]<sup>2-</sup> would lead to an *automatic* cluster expansion; the latter should retain the robust dinuclear Cu<sub>2</sub> motifs of

(19) (a) SMART & SAINT Software Reference manuals, Version 6.45; Bruker Analytical X-ray Systems, Inc.: Madison, WI, 2003. (b) Sheldrick, G. M. SADABS a software for empirical absorption correction, Ver. 2.05; University of Göttingen: Göttingen, Germany, 2002. (c) SHELXTL Reference Manual, Ver. 6.1; Bruker Analytical X-ray Systems, Inc.: Madison, WI, 2000. (d) Sheldrick, G. M. SHELXTL, Ver. 6.12; Bruker AXS Inc.: Madison, WI, 2001. (e) Sheldrick, G. M. SHELXL97, Program for Crystal Structure Refinement; University of Göttingen: Göttingen, Germany, 1997. (f) Bradenburg, K. Diamond, Ver. 3.1eM; Crystal Impact GBR: Bonn, Germany, 2005.

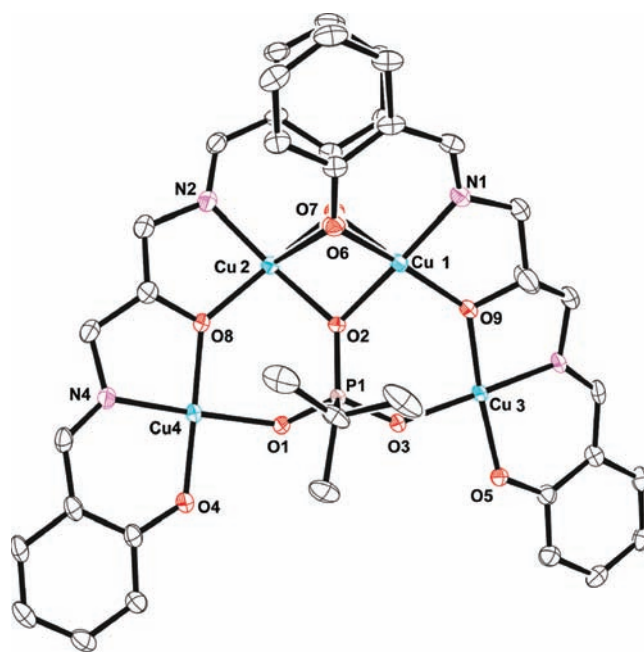
Scheme 2. Synthesis of **5**

the starting precursors. Accordingly a two component reaction involving [Cu<sub>2</sub>(L)(OAc)] or [Cu<sub>2</sub>(L')(OAc)] with RPO<sub>3</sub>H<sub>2</sub> (R = *t*-Bu, Ph, *c*-C<sub>5</sub>H<sub>9</sub>-, *c*-C<sub>6</sub>H<sub>11</sub>-, 2,4,6-*i*-Pr<sub>3</sub>-C<sub>6</sub>H<sub>2</sub>-) was carried out in the presence of triethylamine affording tetranuclear Cu(II) compounds [Cu<sub>4</sub>(L)<sub>2</sub>(*t*-BuPO<sub>3</sub>)](CH<sub>3</sub>OH)<sub>2</sub>(C<sub>6</sub>H<sub>6</sub>) (**1**), [Cu<sub>4</sub>(L)<sub>2</sub>(PhPO<sub>3</sub>)(H<sub>2</sub>O)<sub>2</sub>-(NMe<sub>2</sub>CHO)](H<sub>2</sub>O)<sub>2</sub> (**2**), [Cu<sub>4</sub>(L')<sub>2</sub>(C<sub>5</sub>H<sub>9</sub>PO<sub>3</sub>)](CH<sub>3</sub>-OH)<sub>2</sub> (**3**), [Cu<sub>4</sub>(L')<sub>2</sub>(C<sub>6</sub>H<sub>11</sub>PO<sub>3</sub>)](MeOH)<sub>4</sub>(H<sub>2</sub>O)<sub>2</sub> (**4**) and [Cu<sub>4</sub>(L')<sub>2</sub>(2,4,6-*i*-Pr<sub>3</sub>-C<sub>6</sub>H<sub>2</sub>PO<sub>2</sub>)<sub>2</sub>](PhCH<sub>3</sub>) (**5**) in good yields (Schemes 1 and 2). Interestingly while in **1–4** the phosphonate ligand, [RPO<sub>3</sub>]<sup>2-</sup>, is involved in holding the tetranuclear compound together, in **5**, the tetraanionic anhydride [(RPO<sub>2</sub>)<sub>2</sub>O]<sup>4-</sup>, which is generated in situ, glues the two dinuclear units.

Electronic spectra of these tetranuclear compounds revealed a broad d–d transition in the region of 650 ± 2 nm (**1–4**) and 635 nm (**5**) (see Experimental Section). ESI-MS spectra of the tetranuclear Cu(II) complexes **1–5** reveal that they retain their structures in solution as indicated by the presence of peaks at *m/z* = 980.9617 corresponding to [Cu<sub>4</sub>(L)<sub>2</sub>(*t*-BuPO<sub>3</sub>)]<sup>+</sup> for **1**, *m/z* = 1000.93 corresponding to [Cu<sub>4</sub>(L)<sub>2</sub>(PhPO<sub>3</sub>)]<sup>+</sup> for **2**, *m/z* = 1105.098 for **3** corresponding to [{Cu<sub>4</sub>(L')<sub>2</sub>(C<sub>5</sub>H<sub>9</sub>-PO<sub>3</sub>)]<sup>+</sup>, *m/z* = 1119.11 for **4** corresponding to [{Cu<sub>4</sub>(L')<sub>2</sub>(C<sub>6</sub>H<sub>11</sub>PO<sub>3</sub>)]<sup>+</sup>, and *m/z* = 1505.35 for **5** corresponding to [{Cu<sub>4</sub>(L')<sub>2</sub>(C<sub>30</sub>H<sub>46</sub>P<sub>2</sub>O<sub>5</sub>)]<sup>+</sup>.

**Molecular Structures of 1–5.** The solid-state structures of **1–5** were confirmed by their single crystal X-ray diffraction studies. Crystallographic parameters of these compounds are given in Table 1. All the bond parameters of these compounds are given in Tables S1–S5 in the Supporting Information. Although all the compounds are tetranuclear, there are variations in the structural and compositional details. In compounds **1–4** one [RPO<sub>3</sub>]<sup>2-</sup> is involved in holding the tetranuclear aggregate together. On the other hand in **5** the tetraanionic [(RPO<sub>2</sub>)<sub>2</sub>O]<sup>4-</sup> is involved. Even in **1–4** there are subtle differences; compound **1** belongs to one type while **2–4** belong to another.

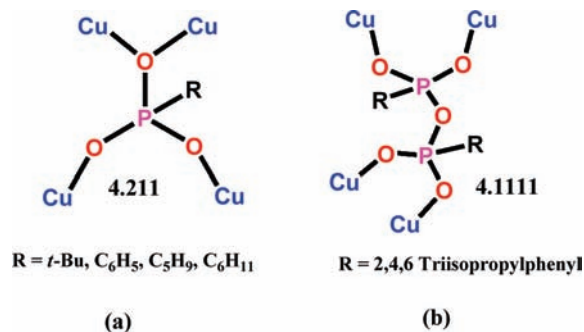
The molecular structure of **1** is shown in Figure 1. An examination of the molecular structure of **1** reveals that the dinuclear motif of the starting material is completely



**Figure 1.** Molecular structure of **1** shown with 50% ellipsoidal probability. Hydrogen atoms are omitted for clarity.

conserved. The two pairs of copper atoms in each dinuclear unit (Cu4 and Cu2; Cu1 and Cu3) (which were bridged by acetate bridges in the starting precursor) are held together by a single [RPO<sub>3</sub>]<sup>2-</sup> ligand in a [4.211]<sup>20</sup> coordination mode (Chart 1). Thus, O2 acts as a single atom bridge between Cu4 and Cu1, while O1 and O3 are coordinated to Cu4 and Cu3. As a result of this coordination, two six-membered rings are simultaneously generated [P1–O1–Cu4–O8–Cu2–O2; P1–O3–Cu3–O9–Cu1–O2]. The P–O distances for the phosphonate ligands are nonequivalent, P(1)–O(1), 1.514(3) Å, P(1)–O(2), 1.553(3) Å and P(1)–O(3), 1.507(3) Å. It can be noted that the longest P–O distance involves O2 which

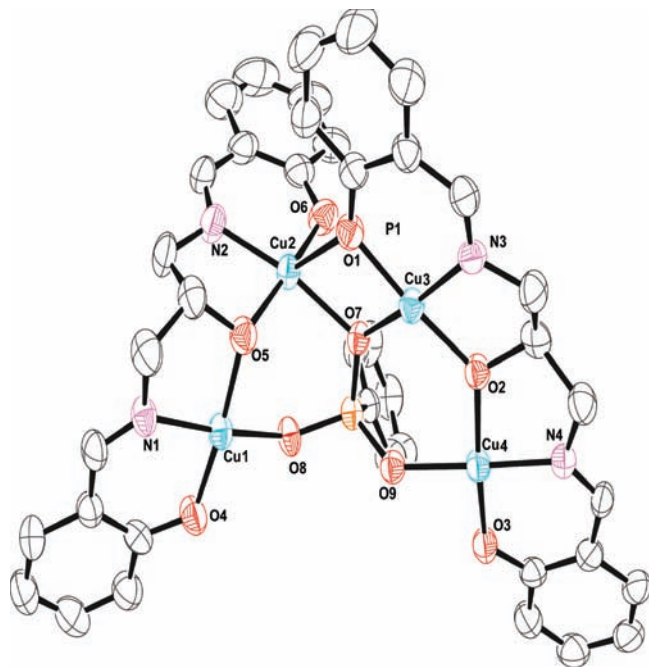
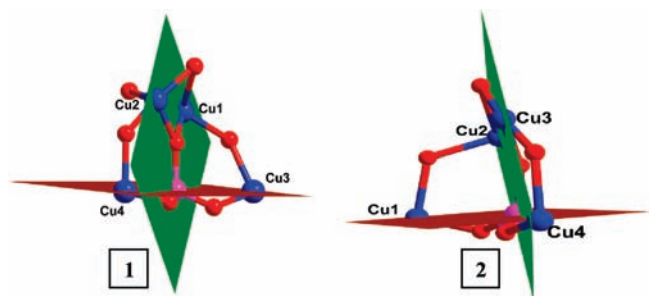
(20) Coxall, R. A.; Harris, S. G.; Henderson, S.; Parsons, S.; Taskar, R. A.; Winpenny, R. E. P. *J. Chem. Soc., Dalton Trans.* **2000**, 14, 2349.

**Chart 1.** Bridging Mode of Phosphonic Acids:<sup>20</sup> (a) Complexes 1–4 and (b) Complex 5

is found to bridge two copper atoms. The phosphonate coordination in **1** forces the phenolate oxygen atoms O7 and O6 to utilize their residual basicity and coordinate to Cu1 and Cu2 respectively. This causes the formation of three puckered four-membered rings [Cu1–O2–Cu2–O6; Cu1–O2–Cu2–O7; Cu1–O6–Cu2–O7]. Among the four copper atoms, Cu1 and Cu2 are five-coordinate (4O, 1N; distorted square pyramidal; apical position occupied by the phenolate oxygen atom O7 or O6) while Cu3 and Cu4 are tetracoordinate (3O, 1N; square planar). The Cu–O bond distances observed in **1** are reasonably similar to each other although the apical Cu–O distances [Cu1–O7 (2.487(2) and Cu2–O6 (2.716(3) Å)] are clearly longer than the others. Among the other Cu–O bond distances, those involving  $\eta^1$  phosphonate oxygen atoms are shorter [Cu3–O3, 1.915(3) Å, and Cu4–O1, 1.935(3) Å] in comparison to the one involved in the bridging mode [Cu1–O2 and Cu2–O2, 1.962(3) (Å)].

Since the molecular structures of **2–4** are quite similar, the structure of **2** is shown as a representative example in Figure 2. The main difference between the structures of **2** and **1** is that in the former only one of the phenolate oxygen atoms exercises its residual basicity and coordinates to the copper atom of the other dinuclear subunit. Thus, Cu3 and Cu1 are bridged by O1, while O6 does not participate in such a coordination action. This is presumably due to the fact that the fifth coordination site on Cu3 is occupied by the water molecule (O14). As a result the central part of the tetranuclear ensemble contains two six-membered rings and only one four-membered ring. All the four copper atoms in **2** are five-coordinate in a distorted square pyramidal geometry. It is to be noticed that the fifth coordination site around Cu1 and Cu4 also is occupied by a solvent molecule (water or dimethylformamide). The coordination environment of the various copper atoms is summarized in Table S6 in the Supporting Information. The two dinuclear segments present in **1** and **2** are nearly orthogonal to each other as illustrated in Figure 3. The molecular structures of **3** and **4** are similar to that of **2** except that in these compounds three of the copper atoms are four-coordinate and square planar while one copper is five-coordinate and distorted square pyramidal (see Figures S1 and S2 in the Supporting Information).

The molecular structure of **5** is different from the others discussed thus far. The two dinuclear segments found in this compound are stitched to each other by the  $[(\text{RPO}_2)_2\text{O}]^{4-}$  ligand (Figure 4). The former is formed in

**Figure 2.** Molecular structure of **2** shown with 50% ellipsoidal probability. Hydrogen atoms are omitted for clarity.**Figure 3.** Representation of the two dinuclear segments of complexes **1** and **2**. The angle between two  $\text{Cu}_2\text{P}$  planes is  $79.804(78)^\circ$  (**1**) and  $84.925(58)^\circ$  (**2**).

situ under the reaction conditions. Precedents for the formation of such species exist in the literature.<sup>21</sup> Each of the two pairs of the  $\text{PO}_2$  units of the phosphonic acid anhydride ligand is involved in bridging two copper atoms of a dinuclear subunit. This coordination mode of the  $\text{PO}_2$  unit is analogous to that of an acetate ligand. The overall coordination mode of the  $[(\text{RPO}_2)_2\text{O}]^{4-}$  ligand is [4.1111] (Chart 1). The P–O bonds involved in the P–O–P unit [O(9)–P(1) and O(9)–P(2): 1.610(3) (Å) and 1.612(3) (Å)] are longer than the remaining P–O bonds [O(7)–P(1), 1.493(3); O(8)–P(1), 1.492(3) (Å); O(10)–P(2), 1.491(3) (Å); and O(11)–P(2), 1.499(3) (Å)]. The flexible P–O–P unit of the  $[(\text{RPO}_2)_2\text{O}]^{4-}$  ligand facilitates the two dinuclear copper units to fold over and to lie nearly on top of each other (Figure 6). Furthermore all the copper atoms in **5** are tetracoordinate and square planar (Table S6 in the Supporting Information). It may be mentioned that the Cu–O bond distances found in the present instance are comparable to that found in the starting dinuclear compound  $[\text{Cu}_2(\text{L})(\text{OAc})]^{15}$

(21) Kingsley, S.; Vij, A.; Chandrasekhar, V. *Inorg. Chem.* **2001**, *40*, 6057.

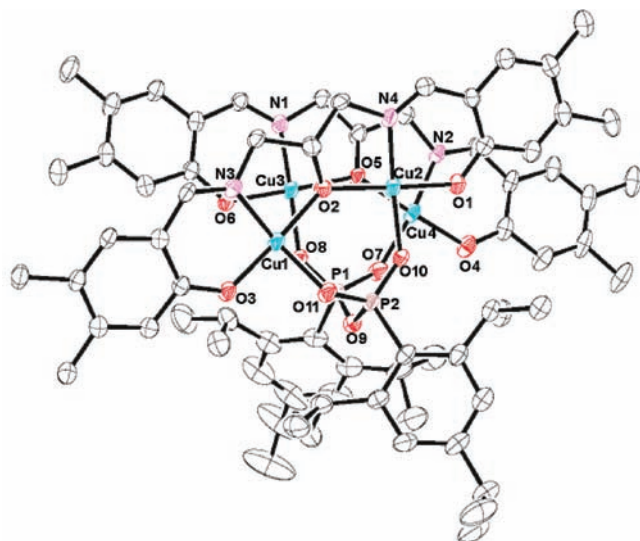


**Figure 4.** Molecular structure of **5** shown with 50% ellipsoidal probability. Hydrogen atoms are omitted for clarity.

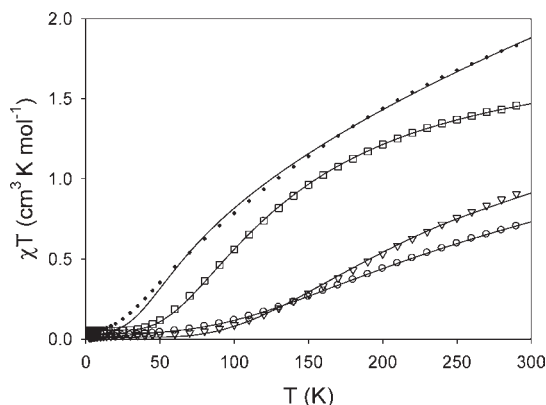


**Figure 5.**  $\chi T$  vs  $T$  plot for complexes **1** (circles), **2** (dots), **3** (triangles) and **5** (squares). The solid line is the best fit; see text for the fitting parameters. The measurement was carried out at an applied field of 1.0 T in the 2 to 300 K temperature range.

Among the tetranuclear copper phosphonates known thus far, several structural types are known as shown for  $[\text{Cu}_4(\mu_3\text{-MePO}_3)_2(\mu\text{-Cl})_2(\text{Cl})_2(3,5\text{-Me}_2\text{PzH})_4]$ ,<sup>8b</sup>  $[\text{Cu}_4(\mu_3\text{-C}_6\text{H}_{11}\text{PO}_3)_2(\mu\text{-Cl})_2(\text{bpy})_4][\text{NO}_3]_2$ ,  $[\text{Cu}_4(\mu_3\text{-C}_6\text{H}_{11}\text{PO}_3)_2(\mu\text{-CH}_3\text{COO})_2(\text{bpy})_4][\text{CH}_3\text{COO}]_2$ , and  $[\text{Cu}_4(\mu_3\text{-C}_5\text{H}_9\text{PO}_3)_2(\mu\text{-Cl})_2(\text{bpa})_4][\text{Cl}_2] \cdot 2\text{MeOH}$  (type I),<sup>8e,j</sup>  $[\text{Cu}_4(\mu_3\text{-C}_6\text{H}_{11}\text{PO}_3)_2(\mu\text{-OH})(\text{bpy})_4(\text{H}_2\text{O})_2][\text{NO}_3]_3$ , and  $\text{Cu}_4(\mu_3\text{-C}_6\text{H}_{11}\text{PO}_3)_2(\mu\text{-OH})(\text{phen})_4(\text{H}_2\text{O})_2][\text{NO}_3]_3$  (type II),<sup>8e,j</sup>  $[\text{Cu}_4(\mu_3\text{-OH})_2(\text{ArPO}_2(\text{OH}))_2(\text{CH}_3\text{COO})_2(3,5\text{-Me}_2\text{PzH})_4][\text{CH}_3\text{COO}]_2 \cdot \text{CH}_2\text{Cl}_2$  (type III),<sup>9c</sup>  $[\text{Cu}_4(3,5\text{-}t\text{-Bu}_2\text{PzH})_4(\mu_3\text{-}t\text{-BuPO}_3)_4]$  (type IV)<sup>8d</sup> and  $[\text{Cu}_4(\text{OH})(\text{Ph}_3\text{CPO}_3)_3\text{-}(\text{Ph}_3\text{PO}_2\text{OH})\text{Py}_4 \cdot \text{H}_2\text{O} \cdot \text{CH}_3\text{CN}]$  (type V)<sup>9a</sup> (Chart 2). The compounds discussed in this study represent new structural types not known hitherto.

**Magnetic Studies.** Magnetic susceptibility data were collected for crushed crystalline samples of **1–3** and **5** (due to structural similarity of complexes **3** and **4**, we carried out the magnetic study only for **3**) at an applied dc field of 1.0 T in the 2 to 300 K temperature range. Additional data were collected at an applied dc field of 500 G below 30 K, where no field dependence was observed.  $\chi T$

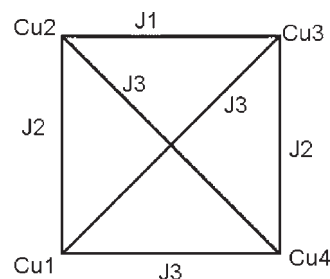


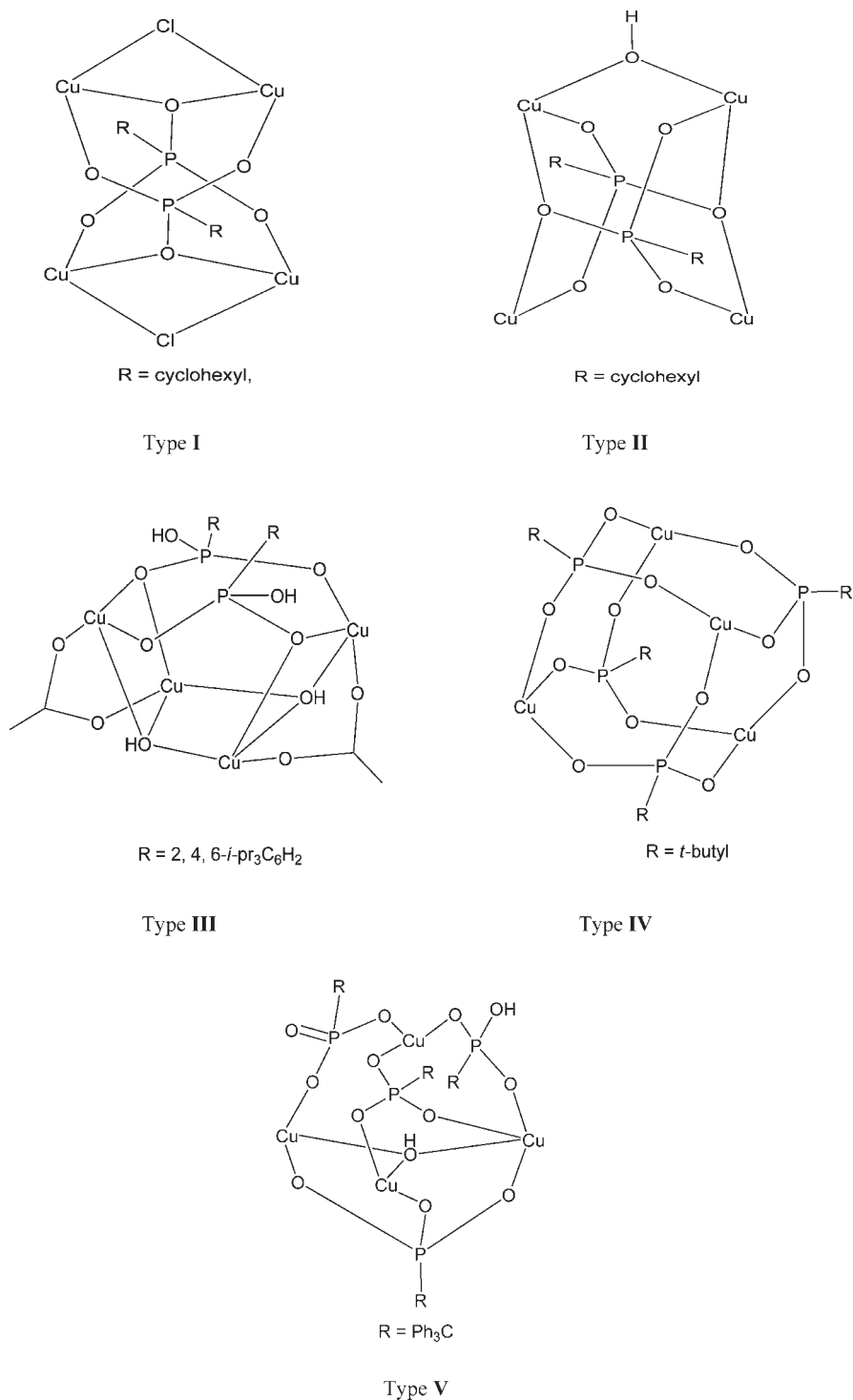
**Figure 6.** Exchange coupling model for complexes **1–5** with the atom numbering used in the spin Hamiltonian.

vs  $T$  plots are shown in Figure 5. The  $\chi T$  value at 300 K for **1** was  $0.76 \text{ cm}^3 \text{ K mol}^{-1}$ , nearly  $1 \text{ cm}^3 \text{ K mol}^{-1}$  below the expected value for four non-interacting Cu(II) ions. This indicates strong antiferromagnetic coupling, and at room temperature, the  $S = 0$  spin ground state is still partly populated. As temperature decreases, so does the  $\chi T$  product, until a plateau is reached below 50 K. The signal becomes very weak at low temperatures, and only the data above 10 K were used to obtain the exchange parameters. The Magpack software<sup>22</sup> which performs the full-matrix diagonalization of the spin matrix, calculated using the spin Hamiltonian  $\hat{H} = -J_1[\hat{S}_2\hat{S}_3] - 2J_2[\hat{S}_1\hat{S}_2 + \hat{S}_3\hat{S}_4] - J_3[\hat{S}_1\hat{S}_3 + \hat{S}_1\hat{S}_4 + \hat{S}_2\hat{S}_4]$ , was used to model the magnetic data following the numbering shown in Figure 6. There are three main exchange pathways, labeled J1, J2 and J3 in Figure 6. The exchange pathways in J1 and J2 are mediated by bridging oxygen atoms of the alkoxide groups of the polydentate ligand ( $\text{C}_{21}\text{H}_{23}\text{N}_2\text{O}_3$ )<sup>3-</sup>, with Cu–O–Cu angles between  $118.05^\circ$  and  $137.15^\circ$  for J2 and Cu–O–Cu angles of  $95.04^\circ$  and  $105.30^\circ$  for J1. For Cu–alkoxide compounds with Cu–O–Cu angles larger than  $95^\circ$  strong antiferromagnetic coupling is expected.<sup>23</sup> However, for J1 one must take into account the fact that the Cu–O–Cu angle of  $95^\circ$  corresponds to an axial–equatorial  $d_{z^2} - d_{x^2 - y^2}$  square interaction, which is expected to afford a weak ferromagnetic coupling,<sup>24</sup> thus the value of J1 will be less antiferromagnetic than expected. Finally, J3 should be antiferromagnetic, as expected for coupling mediated by phosphonate ligands.<sup>9a,b,13h–13l,8d–8k</sup> To avoid overparametrization of the system only one average exchange constant value was used, thus  $J_1 = J_2 = J_3$ . A paramagnetic impurity, probably a Cu(II) salt, was included in the model to fit the experimental data. The best fittings are shown in Figure 5 as a solid line. The fitting parameters for complex **1** were  $J_1 = -74.13 \text{ cm}^{-1}$ , and 0.2% of paramagnetic Cu(II) impurity; the  $g$  was fixed at 2.05, and the agreement between experimental and calculated data was  $F(\text{obj}) = 0.001$ . The  $\chi T$  value at 300 K for **2** was  $1.86 \text{ cm}^3 \text{ K mol}^{-1}$ , above the expected  $1.5 \text{ cm}^3 \text{ K mol}^{-1}$  for four non-interacting Cu(II) ions with  $S = 1/2$  and  $g = 2.0$ . This is due to the presence of a paramagnetic impurity as well as the thermal population of excited states of  $S$  values larger than zero. As temperature decreases, the  $\chi T$  product decreases, indicating strong antiferromagnetic

(22) Borrás-Almenar, J. J.; Clemente-Juan, J. M.; Coronado, E.; Tsukerblat, B. S. *J. Comp. Chem.* **2001**, *2*, 2985 (Magpack Software).

(23) Merz, L.; Haase, W. *J. Chem. Soc., Dalton Trans.* **1980**, 875.

(24) Kahn, O. *Molecular Magnetism*; VCH Publishers: New York, 1993; p 26.

**Chart 2.** Different Tetranuclear Copper Phosphonate Cores Known in the Literature<sup>a</sup>

<sup>a</sup>Carbon, hydrogen and solvent molecules have been deleted for clarity.

coupling within the Cu(II) centers of **2**. As temperature decreases, so does the  $\chi T$  product, until a plateau is reached below 50 K (Figures 5 and S8 in the Supporting Information). The same Hamiltonian used for **1** was used to fit the experimental data with the software package Magpack. The best fitting is shown in Figure 5 as a solid line, and the fitting parameters were  $J_1 = -44.22 \text{ cm}^{-1}$  and 0.7% of paramagnetic Cu(II) impurity with a fixed  $g$  value of 2.05 and  $F(\text{obj}) = 0.0305$ .

The  $\chi T$  product for **3** at 300 K has a value of  $0.94 \text{ cm}^3 \text{ K mol}^{-1}$  per tetranuclear complex, well below the expected  $1.5 \text{ cm}^3 \text{ K mol}^{-1}$  for four non-interacting Cu(II) ions with  $g = 2.0$  and  $S = 1/2$ , indicating strong antiferromagnetic coupling. As temperature decreases, so does the  $\chi T$  product, following a sinusoidal shape that reaches a value near zero below 100 K due to the Boltzmann population of the well-isolated  $S = 0$  spin ground state of **3**. The best simulation of the experimental data was obtained for



$g = 2.2$ , and an average  $J$  value,  $J_1 = -86 \text{ cm}^{-1}$ . A 3% of paramagnetic mononuclear Cu(II) impurity was included in order to model the  $\chi T$  value observed below 50 K. For complex **5** at 300 K the  $\chi T$  product has a value of  $1.47 \text{ cm}^3 \text{ K mol}^{-1}$ , in agreement with the expected  $1.5 \text{ cm}^3 \text{ K mol}^{-1}$  value for four non-interacting Cu(II) ions with  $S = 1/2$ . As temperature decreases, the  $\chi T$  product decreases until it reaches a value of nearly  $0 \text{ cm}^3 \text{ K mol}^{-1}$  below 50 K, as shown in Figure 5 due to the Boltzmann population as temperature decreases of the ground state  $S = 0$  for **5**. Again, there is strong antiferromagnetic coupling between the Cu(II) ions in **5** that leads to an  $S = 0$  spin ground state. The  $\chi T$  product does not reach exactly  $0 \text{ cm}^3 \text{ K mol}^{-1}$  due to the presence of small amount of paramagnetic impurity, probably a Cu(II) compound. Due to the structure of **5** a magnetic model different from that used for **1–3** must be employed. Now only one exchange constant is considered: the main exchange pathway is through the  $\mu$ -oxygen from an alkoxide function of the ligand: O2 bridges Cu1–Cu2 and O5 links Cu3–Cu4 (as labeled in the crystallographic data) through their  $d_{x^2-y^2}$  magnetic orbitals at angles of  $136.12^\circ$  and  $133.96^\circ$ . The oxygen atoms are located in the axial positions of Cu3 and Cu2, leading to an axial–equatorial interaction that should be very weak<sup>24</sup> but the distance between the two dinuclear units formed by Cu1–Cu2 and Cu3–Cu4 is around 2.8 Å, too long to consider this interaction in the model. Thus, complex **5** is taken as two antiferromagnetically coupled  $\text{Cu}_2$  units. The diphosphonate ligands have been proven to provide efficient pathways for magnetic exchange, however, here the magnitude of the exchange through the monatomic oxo bridge dominates the magnetic behavior.<sup>9a,8g,8j</sup> Even though most of the structural correlations relating the Cu–O–Cu angle with the exchange constant are done on  $\text{Cu}_2\text{O}_2$  units with angles smaller than  $110^\circ$ , the results suggest that Cu–O–Cu angles such as those found in **5** would lead

to strong antiferromagnetic coupling.<sup>25</sup> Thus, the magnetic data has been modeled as two  $\text{Cu}_2$  units, using the spin Hamiltonian  $\hat{H} = -2J[S_1 \cdot S_2]$  and writing an analytical Van Vleck equation using the equivalent operator approach. Since the data below 50 K has a value of  $\chi T = 0.05 \text{ cm}^3 \text{ K mol}^{-1}$ , a paramagnetic Cu(II) impurity has been included in the fitting. The best agreement is shown in Figure 5 as a solid line, and the best fitting parameters were  $g = 2.31 \pm 0.02$ ,  $J = -85.7 \pm 0.2 \text{ cm}^{-1}$  and 3% of Cu(II) impurity.

## Conclusion

We have described an approach that can lead to a controlled expansion of a metal aggregate. In this method a dicopper precursor was chosen that contained two distinct types of ligands, a stable Schiff-base ligand platform that held the two copper atoms together and an acetate bridging ligand that could be replaced by other ligands. Accordingly replacing the latter with a phosphonate ligand that possessed an additional oxygen donor site ensured automatic increase in the nuclearity of resulting metal ensemble. The possibility of successfully extending this synthetic principle to other systems depends on the design of the precursor complexes. Currently we are exploring this area.

**Acknowledgment.** We thank the Department of Science and Technology, India, and Council of Scientific and Industrial Research, India, for financial support. V.C. is thankful for the Department of Science and Technology, for a J.C. Bose fellowship. T.S. thanks Council of Scientific and Industrial Research, India, for Senior Research Fellowship. A.D. thanks Council of Scientific and Industrial Research, India, for Senior Research Fellowship.

**Supporting Information Available:** One cif file. Figures S1 and S2 (Diamond pictures of compounds **3** and **4**), Figures S3–S7 (ESI-MS spectra of **1–5**), Figure S8 ( $\chi$  vs  $T$  plots for **1–3** and **5**), Tables S1–S5 (bond parameters of **1–5**), Table S6 (coordination environment of **1–5**). This material is available free of charge via the Internet at <http://pubs.acs.org>.

(25) (a) Merz, L.; Haase, W. *J. Chem. Soc. Dalton* **1980**, 875.  
(b) Thompson, K. L.; Mandal, K. S.; Tandon, S. S.; Bridson, N. J.; Park, K. M. *Inorg. Chem.* **1996**, *35*, 3117.